AD

TECHNICAL REPORT ARCCB-TR-97008

HYDROGEN-INDUCED CRACKING TESTS OF HIGH-STRENGTH STEELS AND NICKEL-IRON BASE ALLOYS USING THE BOLT-LOADED SPECIMEN

G. N. VIGILANTE
J. H. UNDERWOOD
D. CRAYON
S. TAUSCHER
T. SAGE
E. TROIANO

MARCH 1997

US ARMY ARMAMENT RESEARCH, DEVELOPMENT AND ENGINEERING CENTER
CLOSE COMBAT ARMAMENTS CENTER
BENÉT LABORATORIES
WATERVLIET, N.Y. 12189-4050

APPROVED FOR PUBLIC RELEASE; DISTRIBUTION UNLIMITED

DISCLAIMER

The findings in this report are not to be construed as an official Department of the Army position unless so designated by other authorized documents.

The use of trade name(s) and/or manufacturer(s) does not constitute an official indorsement or approval.

DESTRUCTION NOTICE

For classified documents, follow the procedures in DoD 5200.22-M, Industrial Security Manual, Section II-19 or DoD 5200.1-R, Information Security Program Regulation, Chapter IX.

For unclassified, limited documents, destroy by any method that will prevent disclosure of contents or reconstruction of the document.

For unclassified, unlimited documents, destroy when the report is no longer needed. Do not return it to the originator.

REPORT DOCUMENTATION PAGE

Form Approved
OMB No. 0704-0188

1. AGENCY USE ONLY (Leave blank)	2. REPORT DATE	3. REPORT TYPE AND DATES COVERED
	March 1997	Final

4. TITLE AND SUBTITLE
HYDROGEN-INDUCED CRACKING TESTS OF HIGH-STRENGTH STEELS AND NICKEL-IRON BASE ALLOYS USING THE BOLT-LOADED SPECIMEN

5. FUNDING NUMBERS
AMCMS No. 6111.01.91A1.1

6. AUTHOR(S)

G.N. Vigilante, J.H. Underwood, D. Crayon,
S. Tauscher, T. Sage, and E. Troiano

7. PERFORMING ORGANIZATION NAME(S) AND ADDRESS(ES)

U.S. Army ARDEC
Benet Laboratories, AMSTA-AR-CCB-O
Watervliet, NY 12189-4050

8. PERFORMING ORGANIZATION REPORT NUMBER
ARCCB-TR-97008

9. SPONSORING / MONITORING AGENCY NAME(S) AND ADDRESS(ES)

U.S. Army ARDEC
Close Combat Armaments Center
Picatinny Arsenal, NJ 07806-5000

10. SPONSORING / MONITORING AGENCY REPORT NUMBER

11. SUPPLEMENTARY NOTES

Presented at the ASTM 28th National Symposium on Fatigue and Fracture Mechanics, Saratoga Springs, NY, 25-27 June 1996.
Published in *ASTM STP 1321. Fatigue and Fracture Mechanics, 28th Volume.*

12a. DISTRIBUTION / AVAILABILITY STATEMENT

Approved for public release; distribution unlimited.

12b. DISTRIBUTION CODE

13. ABSTRACT *(Maximum 200 words)*

Hydrogen-induced cracking tests were conducted on high-strength steels and nickel-iron base alloys using the constant displacement bolt-loaded compact specimen. The bolt-loaded specimen was subjected to both acid and electrochemical cell environments to produce hydrogen. The materials tested were A723, Maraging 200, PH 13-8 Mo, Alloy 718, Alloy 706, and A286, ranging in yield strength from 760-1400 MPa. The effects of chemical composition, refinement, heat treatment, and strength on hydrogen-induced crack growth rates and thresholds were examined. In general, all high strength steels tested exhibited similar crack growth rates and threshold levels. In comparison, the nickel-iron base alloys tested exhibited crack growth rates up to three orders of magnitude lower than the high-strength steels tested. It is widely known that high-strength steels and nickel base alloys exhibit different crack growth rates, in part, because of their different crystal cell structure. In the high-strength steels tested, refinement and heat treatment had some effect on hydrogen-induced cracking, although strength was the predominant factor influencing susceptibility to cracking. When the yield strength of one of the high-strength steels tested was increased moderately, from 1130 MPa to 1275 MPa, the incubation times decreased by over two orders of magnitude, the crack growth rates increased by an order of magnitude, and the threshold stress intensity was slightly lower.

14. SUBJECT TERMS
Threshold Stress Intensity, Hydrogen-Induced Cracking, Hydrogen Cracking, Hydrogen Embrittlement, Environmental Fracture, Environmental Cracking, Crack Growth Rates, High-Strength Steels, Nickel-Iron Base Alloys

15. NUMBER OF PAGES
21

16. PRICE CODE

17. SECURITY CLASSIFICATION OF REPORT	18. SECURITY CLASSIFICATION OF THIS PAGE	19. SECURITY CLASSIFICATION OF ABSTRACT	20. LIMITATION OF ABSTRACT
UNCLASSIFIED	UNCLASSIFIED	UNCLASSIFIED	UL

TABLE OF CONTENTS

List of Tables

List of Figures

ACKNOWLEDGMENTS

Thanks to Mr. A. Kapusta for fractography of the bolt-loaded specimens.

INTRODUCTION

Hydrogen-induced cracking failures have been a particular problem in applications involving high-strength materials in aggressive service environments, including armament applications. Recently, a 1.7-m long crack was found at an outside diameter keyway of a gun tube. An investigation concluded that hydrogen stress cracking occurred at a location of tensile residual stress after being exposed to an aggressive electropolish solution.[1] Also, higher energy propellants have been shown to increase the risk of hydrogen damage to bore coatings, liners, and the underlying steel substrate.[2] In addition, Troiano et al.[3] have concluded that premature seal failures in armament were likely caused by the hydrogen-rich byproducts of the combustion environment.

In this work, a fracture mechanics approach was used to measure the hydrogen-induced cracking threshold of various steels and nickel-iron base alloys at various yield strength levels. The effects of refinement were also examined for one of the steels tested. The constant displacement bolt-loaded compact sample (Figure 1), henceforth referred to as "the bolt-loaded sample," was used in the testing because it provides quantitative information on the crack growth rate, da/dt, and the threshold stress intensity, K_{IHIC}, in a simple test. K_{IHIC} is the threshold stress intensity under which no cracking will occur in a given material in a hydrogen environment. As a crack grows in a bolt-loaded specimen, the load, and therefore the stress intensity, decreases until K_{IHIC} is reached. This test is fundamentally different from constant load tests, where K_{IHIC} is found by testing several specimens at various initial stress intensities until no cracking occurs. One disadvantage of the bolt-loaded specimen is that long test times (up to 10,000 hours) may be necessary when testing insensitive materials, nonaggressive environments, and at low initial stress intensities. This problem may be mitigated by first testing a sample at a high initial stress intensity level approaching K_{IC}. This will aid in determining material susceptibility and the initial applied stress intensity levels for subsequent tests. There is currently no recognized standardization of the bolt-loaded specimen; however, an ASTM committee is incorporating a bolt-loaded compact specimen standard with the recently adopted ASTM standard E 1681-95 on environment-assisted cracking.

MATERIALS AND ENVIRONMENTS

Materials

The materials used in this investigation consisted of martensitic and austenitic-forged alloys with yield strengths ranging from 760 to1400 MPa. The martensitic alloys used have a body-centered cubic (BCC) crystal structure, and the austenitic materials have a face-centered cubic (FCC) crystal structure. The materials investigated were A723, Maraging 200, PH 13-8 Mo steels, Alloy 718, Alloy 706 nickel-iron base alloys, and A286 iron-nickel base alloy. The materials A723, Maraging 200, and PH 13-8 Mo were chosen for their high strength and toughness properties (in air). Alloys 718 and 706 were chosen for their high strength, crystal structure, and hydrogen-induced cracking resistance (compared with the steels tested).[4,5] Alloy A286 was chosen for its well-known resistance to hydrogen-induced cracking.[6,7] Some pertinent mechanical/material properties of the tested materials are listed in Table 1.

The material A723 is a Ni-Cr-Mo quenched and tempered steel. Both A723 Grade 1 and Grade 2 compositions were evaluated to determine the effects of strength, composition, and refinement on da/dt and K_{IHIC}. All A723 materials tested had an ASTM grain size of 11.8. The A723 Grade 1 material was electric furnace melted and vacuum degassed (EFM-VD). The A723 Grade 2 material was either electric furnace melted and electro-slag remelted (EFM-ESR) or vacuum induction melted and vacuum arc remelted (VIM-VAR). Both the ESR and VIM-VAR refinement methods increase the homogeneity of the microstructure and reduce the amount of sulfur (S) and phosphorus (P) present compared with the EFM-VD condition. The levels of S and P in the Grade 1, Grade 2 (ESR), and Grade 2 (VIM-VAR) steels were 0.005/0.006, 0.002/0.005, and 0.0007/0.005, respectively. Additionally, the Grade 2 material contained slightly more Ni to improve fracture toughness. Maraging 200 is an 18Co-8Ni steel that was conventionally austenitized and aged to promote strengthening by Ni_3[Ti, Mo, Al] precipitates. The Maraging 200 material tested had an ASTM grain size of 13.5. PH 13-8 Mo is a 13Cr-8Ni-2Mo martensitic stainless-steel that was heat-treated to two standard overaged conditions. PH 13-8 Mo is strengthened by NiAl precipitates during the aging process. The ASTM grain size of the PH 13-8 Mo material investigated was 8.6. Alloy 718 is a 52Ni-19Cr-19Fe superalloy that was tested in the direct-aged condition for maximum strength and a standard heat treatment condition for maximum ductility and impact strength.[8] Alloy 718 receives its strength from Ni_3Nb (γ'') precipitates. Alloy 718 in the direct-aged condition had an ASTM grain size of 8.6 while the conventionally processed 718 had a grain size of 7.0. Alloy 706 is a 41Ni-38Fe-16Cr superalloy tested in a standard heat-treated condition to maximize ductility and impact strength and to promote formation of Ni_3[Nb, Ti, Al] (γ') precipitates.[9] The Alloy 706 material tested had an ASTM grain size of 5.3. A286 is an Fe-25Ni-15Cr superalloy that was tested in a standard heat treatment condition. A286 is also precipitation strengthened by γ'. The ASTM grain size for the A286 material tested was 10.6. Table 2 lists the various heat treatments of the materials tested.

Environments

All tests were conducted in either electrochemical cells or in concentrated acid solutions, with the exception of A723 Grade 1 (1160 MPa YS) and Grade 2 (1130 MPa YS) and Alloy 706, which were tested in both environments. All tests were conducted at ambient temperature.

The electrochemical cell tests were conducted using a platinum anode and specimen cathode in a 3.5% aqueous NaCl solution. As_2O_3 was used as a "poison" to limit the combination of nascent hydrogen to the diatomic gas.[10] All specimens tested using this method were precharged at a current density of 40 ma/cm^2 for 8 hours prior to load application. A current density of 40 ma/cm^2 was also applied during testing. This current density was maintained at a constant value by using a current-controlling power source and keeping the exposed surface area of the specimen constant throughout the test. The NaCl solution volume was monitored daily to ensure a constant current density and replaced weekly to ensure a constant reservoir chemistry.

All acid cracking tests were conducted in a concentrated 50% sulfuric acid and 50% phosphoric acid solution (by volume). This solution is identical to that used in previous tests.[1]

TEST PROCEDURE

All bolt-loaded test specimens were taken in the C-R orientation as described in ASTM E 399. All tests were conducted following interlaboratory guidelines on the bolt-loaded specimen from Wei and Novak.[11] All A723 steels tested in acid were tested in triplicate for each test condition. All bolt-loaded tests were tested at an initial stress intensity of 55 MPa√m, with the exception of one Alloy 706 specimen, which was tested at 110 MPa√m. The low-stress intensities of 55 MPa√m were chosen from previous experience to avoid the problem of a deep crack growing too near to the back edge of the specimen. All tests were conducted in acid or an electrochemical cell, as described in the preceding section. The stress intensity in the bolt-loaded sample is related to the mouth opening through the following relationship:[1]

$$K_{applied} = f(a/W) E v (1 - a/W)^{1/2} \; / \; W^{1/2} \qquad 1$$

$$f(a/W) = 0.654 - 1.88(a/W) + 2.66(a/W)^2 - 1.233(a/W)^3$$

where v is mouth opening and E is Young's modulus. This K expression is valid for $0.3 \leq a/W \leq 1$. For the acid cracking tests, the acid was introduced to the crack tip prior to load application to expose fresh surfaces produced by the subsequent loading. The crack extension of the specimens was monitored optically on both specimen sides on a regular basis to determine $K_{applied}$ as a function of time and to obtain da/dt information. The mouth opening of the test specimen and the solution pH were checked frequently to ensure no relaxation or solution contamination, respectively. The duration of the tests depended on the material tested and its yield strength. Typically, tests were conducted for durations ranging from 1500 to 6000 hours. After test completion, the final crack length was measured to determine if the test conformed to plain-strain test conditions, and the fracture surface was examined visually and by scanning electron microscopy to determine the fracture morphology. From previous experience it is believed that all materials would easily conform to plane-strain conditions because of low hydrogen-induced cracking threshold values.

RESULTS AND DISCUSSION

In general, the BCC materials tested exhibited similar cracking characteristics. Both da/dt and K_{IHIC} information was similar, although both the PH 13-8 Mo materials tested had lower crack growth rates and slightly higher K_{IHIC} than the average BCC materials tested. The FCC materials tested had a lower crack growth rate than the BCC materials. This was expected in part because diffusivity of hydrogen through an open-cell BCC structure is higher than through a closed-cell FCC structure. In other research, crack growth rates have been shown to be orders of magnitude less in FCC structures than in BCC structures (e.g., Ritchie et al.[12]).

The following sections discuss the results of the various materials tested. Table 3 summarizes the results of the hydrogen-induced cracking tests conducted on all materials.

A723 Steel

The hydrogen-induced cracking tests conducted on A723 steels in acid environments showed dramatic results when plotted as applied stress intensity versus time (Figure 2). Figure 2 shows the trend of the data, illustrating the incubation time, subsequent crack growth, and threshold. Although the Grade 1 and Grade 2 materials were tested at about the same yield strength level (1160 and 1130 MPa, respectively), the incubation time increased from approximately 200 hours to more than 2,000 hours. Additionally, when the yield strength of the Grade 2 material was increased 13% from 1130 MPa to 1275 MPa, the incubation time decreased over two orders of magnitude (i.e., from more than 2,000 hours to less than 12 hours). After the incubation time was exceeded, the crack grew until K_{IHIC} was reached. Incubation time has been observed to decrease with an increase in strength or applied stress (e.g., Steigerwald et al.[13] and Jones[14]). However, both the strength and applied stress intensity levels were nearly identical in the lower yield strength Grade 1 and Grade 2 materials tested. This suggests that the local crack tip chemistry may have been the controlling factor. Therefore, the longer incubation time of the lower strength Grade 2 material may be attributed to the refinement and increased Ni content as compared with the Grade 1 material.

The crack growth rates of the A723 steels conducted in acid are shown in Figure 3. A five-point moving average was used to analyze the data. This curve shows the stage I and a portion of the stage II crack growth regimes. For the lower strength Grade 1 and Grade 2 steels, da/dt in the stage II regime appears to be constant at approximately 10^{-5} mm/s, the same as that found by Underwood et al.[1] The constant da/dt data in the stage II regime for the lower strength steels are independent of K and are solely a result of diffusion-controlled crack growth. For the higher strength Grade 2 steel, the da/dt in the stage II regime were approximately an order of magnitude higher (10^{-4} mm/s). Note the wide scatter in both of the lower strength steels at the initial applied stress intensity of 55 MPa$\sqrt{m}$. This scatter occurred during the incubation period when little or no crack growth was observed. After incubation, the crack grew significantly and the scatter was eliminated. The average K_{IHIC} for the lower strength Grade 1 steel was approximately 16 MPa$\sqrt{m}$. The average K_{IHIC} for the higher strength ESR and VIM-VAR processed Grade 2 materials was approximately 10 and 11 MPa$\sqrt{m}$, respectively.

The electrochemical cell tests on the lower strength Grade 1 and Grade 2 steels exhibited incubation times of approximately 325 and 450 hours, respectively, then cracked rapidly and reached K_{IHIC} levels of approximately 10 and 16 MPa$\sqrt{m}$, respectively. Figure 4 shows the applied stress intensity as a function of exposure time for all materials tested in the electrochemical cell tests. In the electrochemical cell tests, little distinction showed in the incubation time between the Grade 1 and Grade 2 steels tested. It is believed that the high-current density liberated more hydrogen than the acid tests, thereby increasing the severity of cracking in both steels and reducing the incubation time in the Grade 2 steel. If the current density were decreased significantly, a more notable distinction may have been apparent. Also, only the A723 steels tested in the electrochemical cell exhibited a classical incubation period. This appears to more than just a strength effect, because the 1035 MPa yield strength PH 13-8 Mo material tested did not exhibit an incubation time.

The crack growth rates of the A723 steels tested in the electrochemical cell were approximately 10^{-5} mm/s, as seen in Figure 5. A five-point moving average was used to plot the data. In Figure 5, the initial scatter was omitted from the A723 steels for clarity.

The fracture surface near the crack tip of the higher strength ESR-processed Grade 2 material is shown in Figure 6a. In this figure, the intergranular fracture morphology is evident, as is the chemical attack of the fracture surface caused by the acid solution. Much more chemical attack was observed at lower a/W values, as would be expected due to longer exposure to the acid. The remaining ligament of this specimen was forced open by tensile overload after testing was completed. Figure 6b shows a predominantly ductile fracture morphology of microvoid coalescence. However, the island of intergranular fracture is believed to have resulted from the remaining ligament being embrittled by hydrogen during immersion in the acid solution. When the tensile load was applied to break the remaining ligament, a portion of it failed in a brittle, intergranular manner.

There were little differences in the S and P content in the A723 steels examined between the EFM-VD and EFM-ESR refinement methods. The VIM-VAR-processed steel contained approximately the same amount of P and much less S than either the VD or ESR-processed steels. Because the S is "tied up" as manganese sulfide stringers in A723 steels and the P content remained essentially constant, no direct correlation can be made here on the effects of these impurities on incubation time, da/dt, or K_{IHIC}. Previous studies have shown no strong effect of impurities on hydrogen-induced cracking of high-strength steels with yield strength greater than 1250 MPa.[15]

PH 13-8 Mo

The PH 13-8 Mo material tested in the 1275 MPa yield strength condition resulted in a K_{IHIC} value of approximately 17 MPa$\sqrt{m}$. The material tested at a lower yield strength level of 1035 MPa resulted in a K_{IHIC} value of approximately 19 MPa$\sqrt{m}$. It was surprising that the lower yield strength condition did not provide a more improved K_{IHIC}. More dramatic threshold results may have been gained if the PH 13-8 Mo material were tested in a peak-aged and an overaged condition rather than two overaged conditions because the mechanical properties from a highly overaged condition result in lower strength as well as toughness due to precipitate incoherency. Fracture toughness tests by Young et al.[16] on H-charged PH 13-8 Mo specimens at a yield strength level of 1275 MPa show results similar to those obtained in these tests.

Maraging 200

The Maraging 200 material tested in the electrochemical cell exhibited a K_{IHIC} value of approximately 13 MPa$\sqrt{m}$.

Alloy 718

The Alloy 718 material tested in the direct-aged condition exhibited no distinctive incubation time. As seen in Figure 4, the crack grew much slower and did not exhibit any gross crack advances as with the BCC materials, an advantage attributed to the lower diffusivity of H

through the FCC crystal structure. However, K_{IHIC} for the direct-aged Alloy 718 specimen was similar or less than that of the BCC materials tested. The lower than expected yield strength and low K_{IHIC} values were attributable to an undesirable δ phase present at the grain boundaries.[17] Figure 7a shows the fracture surface in the cracked portion of the Alloy 718 material tested in the direct-aged condition. The fracture surface is entirely intergranular in nature, with evidence of the second phase present at the grain boundaries. Figure 7b shows the fracture surface of the ruptured remaining ligament. The fracture morphology is brittle, containing both quasi-cleavage and intergranular fracture.

The Alloy 718 material that was heat-treated to provide maximum ductility and impact strength exhibited no appreciable cracking after 5,000 hours of exposure. The K_{IHIC} of Alloy 718 in this condition could be as high as 42 MPa√m, based on environmental fracture tests conducted by Walter and Chandler.[4]

Alloy 706

After more than 3,000 hours in acid and 5,000 hours in the electrochemical cell, no appreciable cracking was observed in the Alloy 706 specimens at both the 55 MPa√m and 110 MPa√m initial applied stress intensity levels. For example, after 5,000 hours of exposure in the electrochemical cell at an initial applied stress intensity of 110 MPa√m, the current applied stress intensity was 90 MPa√m, which corresponded to crack growth of only approximately 3.7 mm. It is believed that the K_{IHIC} value of Alloy 706 will be higher than that of Alloy 718 because slow strain rate notched tensile tests conducted on both alloys showed a higher notched tensile strength ratio for Alloy 706 than for Alloy 718.[18] The slow strain rate notched tensile tests were conducted on specimens that were hydrogen-charged and compared with control specimens tested in laboratory air. The notched tensile strength ratio of the Alloy 706 specimens was 0.91 compared with 0.84 for the Alloy 718 specimens. High-pressure hydrogen-notched tensile tests also showed a higher ratio for Alloy 706 than for Alloy 718.[4]

A286

After more than 2,300 hours in the electrochemical cell, no visible cracking occurred with the A286 material. The K_{IHIC} value is expected to be higher than that of Alloys 718 and 706 because slow strain rate notched tensile tests showed a ratio of 0.98 for A286 compared with 0.84 and 0.91, for Alloys 718 and 706, respectively.[18] High-pressure hydrogen-notched tensile tests conducted on A286 also showed an improved resistance to hydrogen compared with Alloys 718 and 706.[4]

SUMMARY AND CONCLUSIONS

1. Hydrogen-induced cracking studies were conducted on A723, Maraging 200, PH 13-8 Mo, Alloy 718 Direct-Aged, Alloy 718, Alloy 706, and A286 alloys using the constant displacement bolt-loaded compact specimen. All tests were conducted in either 50% sulfuric-50% phosphoric acid solutions or in electrochemical cells at room temperature. All tests, with the exception of Alloy 706, were conducted at initial stress intensities of 55 MPa√m. Information on crack growth rates and hydrogen-induced cracking threshold

stress intensities (with the exception of Alloys 718, 706, and A286) was obtained from these tests.

2. The bolt-loaded specimen has provided closely repeatable hydrogen-induced cracking tests and allows for accurate crack growth rate and threshold measurement.

3. With the lower strength A723 steels tested in an acid environment, an incubation period was observed followed by crack growth and asymptotic approach of a threshold. At the lower strength levels (e.g., 1130 MPa YS) refinement and alloying had an effect on the hydrogen-induced cracking susceptibility of A723; however, at high-strength levels (1275 MPa YS), no benefit is apparent. In A723, yield strength had the most pronounced effect on hydrogen-induced cracking susceptibility. As the strength of A723 increased, the incubation time and K_{IHIC} decreased while the crack growth rate increased. Crack growth rates in the stage II cracking regime for the lower strength A723 Grade 1 steel were approximately 10^{-5} mm/s. Crack growth rates in the stage II regime for the higher strength Grade 2 steels were about an order of magnitude larger.

4. The electrochemical tests were more severe than the acid cracking tests for A723 steel. A shorter incubation time was observed for the A723 Grade 2 steel, and a lower threshold was evident for both Grade 1 and Grade 2 steels tested in the electrochemical cell.

5. Alloy 718 tested in the direct-aged condition had a low K_{IHIC} value of 11 MPa$\sqrt{m}$, which is attributable to a deleterious δ phase present at the grain boundaries. Alloy 718 tested under a standard high ductility heat treatment condition was much more resistant to hydrogen-induced cracking because no cracking was observed after 5,000 hours of exposure.

6. A286 and Alloy 706 have not exhibited any measurable crack growth in bolt-loaded tests conducted at 55 MPa$\sqrt{m}$ after 2,400 and 3,000 hours of exposure, respectively. Although Alloy 706 tested at 110 MPa$\sqrt{m}$ showed a small amount of crack extension after 5,000 hours of exposure, it has proven to be very resilient to hydrogen-induced cracking.

7. The martensitic materials tested in this investigation exhibited similar crack growth rates and hydrogen-induced cracking threshold stress intensity values, with the exception of the two PH 13-8 Mo specimens tested at 1130 MPa YS and 1275 MPa YS, which had slightly lower crack growth rates.

8. The austenitic materials tested in this investigation exhibited up to three orders of magnitude lower crack growth rates than the martensitic materials tested.

REFERENCES

1. Underwood, J. H., Olmstead, V. J., Askew, J. C., Kapusta, A. K., and Young, G. A., "Environmentally Controlled Fracture of an Overstrained A723 Steel Thick-Wall Cylinder," *ASTM STP 1189*, American Society for Testing and Materials, Philadelphia, 1993, pp. 443-460.

2. Dalley, A. M., Buckman, R. W. Jr., and Bagnall, C., "Physical and Chemical Interactions at the Bore Surface of a Ta-10W Gun Barrel Liner," *MPIF-APMI International Conference on Tungsten and Refractory Metals, Their Alloys, Composites and Carbides*, Washington DC, November 1995.

3. Troiano, E., Underwood, J. H., Scalise, A., O'Hara, G. P., and Crayon, D., "Fatigue Analysis of a Vessel Experiencing Pressure Oscillations," *Fatigue and Fracture Mechanics: 28th Volume, ASTM STP 1321*, (J. H. Underwood, B. D. MacDonald, M. R. Mitchell, Eds.), American Society for Testing and Materials, Philadelphia, 1997.

4. Walter, R. J. and Chandler, W. T., "Influence of Gaseous Hydrogen on Inconel 718," *Hydrogen in Metals*, 1974, pp. 515-524.

5. *Handbook of Corrosion Data*, ASM International Materials Data Series, 1989, p. 333.

6. Thompson, A. W. and Brooks, J. A., "Hydrogen Performance of Precipitation-Strengthened Stainless Steels Based on A-286," *Metallurgical Transactions A*, Vol. 6A, July 1975, pp. 1431-1442.

7. Papp, J., Hehemann, R. F., and Troiano, A. R., "Hydrogen Embrittlement of High Strength FCC Alloys," *Hydrogen in Metals*, 1974, pp. 657-669.

8. Inco Alloys International, Product Literature on Inconel Alloy 718, 1968.

9. Huntington Alloys, Inc., Product Literature on Inconel Alloy 706, 1974.

10. Spencer, G. L., "Hydrogen Embrittlement of Gun Steel," Master's Thesis, Rensselaer Polytechnic Institute, Troy, NY, August 1987.

11. Wei, R. P. and Novak, S. R., "Interlaboratory Evaluation to K_{ISCC} and da/dt Determination Procedures for High-Strength Steels," *Journal of Testing and Evaluation*, Vol. 15, No. 1, January 1987.

12. Ritchie, R. O., Castro Cedeño, M. H., Zackay, V. F., and Parker, E. R., "Effects of Silicon Additions and Retained Austenite on Stress Corrosion Cracking in Ultrahigh Strength Steels," *Metallurgical Transactions A*, Vol. 9A, 1978, pp. 35-40.

13. Steigerwald, E. A., Schaller, F. W., and Troiano, A. R., "The Role of Stress in Hydrogen Induced Delayed Failure," *AIME Transactions*, Vol. 218, October 1960, pp. 832-841.

14. Jones, D. A., *Principles and Prevention of Corrosion*, Prentice Hall, Inc., Saddle River, NJ, 1996, p. 249.

15. Craig, B., "Limitations of Alloying to Improve the Threshold for Hydrogen Stress Cracking of Steels," *Hydrogen Effects on Material Behavior*, 1989, pp. 955-963.

16. Young, L. M., Eggleston, M. R., Solomon, H. D., and Kaisand, L. R., "Hydrogen-Assisted Cracking in a Precipitation Hardening Stainless Steel: Effects of Heat Treatment and Displacement Rate," *Materials Science and Engineering*, 1995, pp. 377-387.

17. Vigilante, G. N. and Fusco, D. R., "Evaluation of High Strength Materials for the Regenerative Liquid Propellant Gun Program," ARDEC Technical Report #95035, Benet Laboratories, Watervliet, NY, August 1995.

18. Tauscher, S. and Sage, T., Unpublished Research, 1995.

Table 1. Mechanical/material property information on the materials tested

Material	Yield Strength (MPa)	Fracture Toughness (MPa√m)	Crystal Structure
A723 Grade 1	1160	125	BCC
A723 Grade 2 (ESR)	1130	175	BCC
A723 Grade 2 (ESR)	1275	125	BCC
A723 Grade 2 (VIM-VAR)	1275	170	BCC
Maraging 200	1400	175	BCC
PH 13-8 Mo	1275	145	BCC
PH 13-8 Mo	1035	125	BCC
Alloy 718 (Direct-Aged)	1150	135	FCC
Alloy 718	1115	145	FCC
Alloy 706	1110	180	FCC
A286	760	125	FCC

Table 2. Heat treatments of materials tested

Materials	Heat Treatment
A723 Grade 1 @ 1160 MPa YS	843°C 1 hour Water Quench, Temper 582°C 4 hours Air Cool
A723 Grade 2 @ 1130 MPa YS	843°C 1 hour Water Quench, Temper 627°C 4 hours Air Cool
A723 Grade 2 @ 1275 MPa YS	843°C 1 hour Water Quench, Temper 524°C 4 hours Air Cool
PH 13-8 Mo @ 1275 MPa YS	927°C 1/2 hour Air Cool, Refrigerate -73°C, 2 hours Air Warm, Age 556°C 4 hours Air Cool
PH 13-8 Mo @ 1035 MPa YS	927°C 1/2 hour Air Cool, Refrigerate -73°C, 2 hours Air Warm, Age 579°C 4 hours Air Cool
Maraging 200	816°C 1 hour Water Quench, Age 482°C 3 hours Air Cool
Alloy 718 Direct-Aged	718°C 8 hours Furnace Cool to 621°C 18 hours Air Cool
Alloy 718	1038°C 1/3 hour Air Cool, Age 760°C 11 hours Furnace Cool to 649°C 9 hours Air Cool
Alloy 706	982°C 1 hour Air Cool, Age 718°C 8 hours Furnace Cool 38°C/hour to 621°C 8 hours Air Cool
A286	816°C 1 hour Water Quench, Age 718°C 16 hours Air Cool

Table 3. Summary of K_{IHIC} test results

Material	Yield Strength (MPa)	K_{IHIC} (MPa$\sqrt{m}$)	Test Environment
A723 Grade 1	1160	16/10	acid/cell
A723 Grade 2 (ESR)	1130	16/16	acid/cell
A723 Grade 2 (ESR)	1275	12	acid
A723 Grade 2 (VIM-VAR)	1275	12	acid
Maraging 200	1400	12	cell
PH 13-8 Mo	1275	17	cell
PH 13-8 Mo	1035	19	cell
Alloy 718	1150	11	cell
Alloy 718	1115	-	cell
Alloy 706	1110	-	acid/cell
A286	760	-	cell

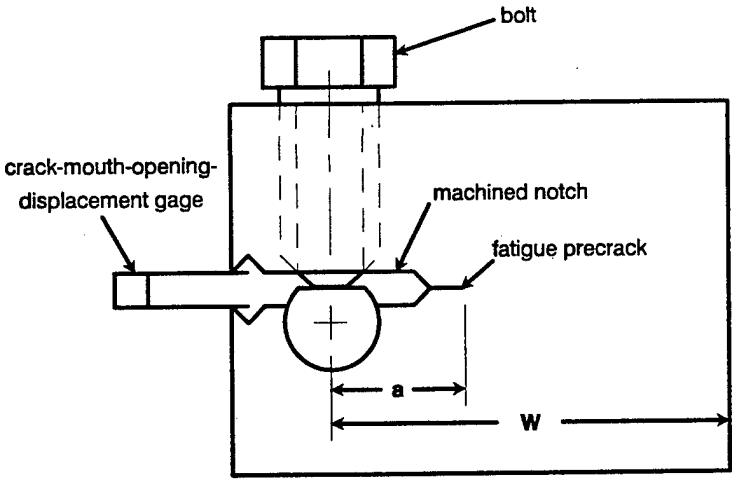

Figure 1. Schematic of bolt-loaded test specimen

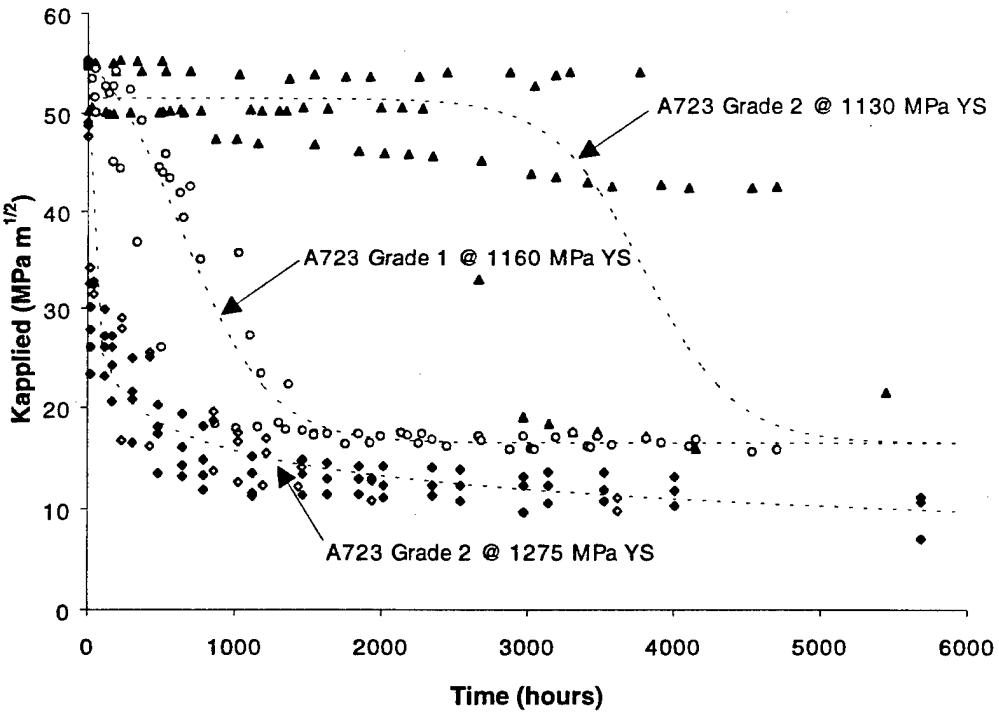

Figure 2. Applied K versus time for A723 steels exposed to a 50% sulfuric - 50% phosphoric acid solution

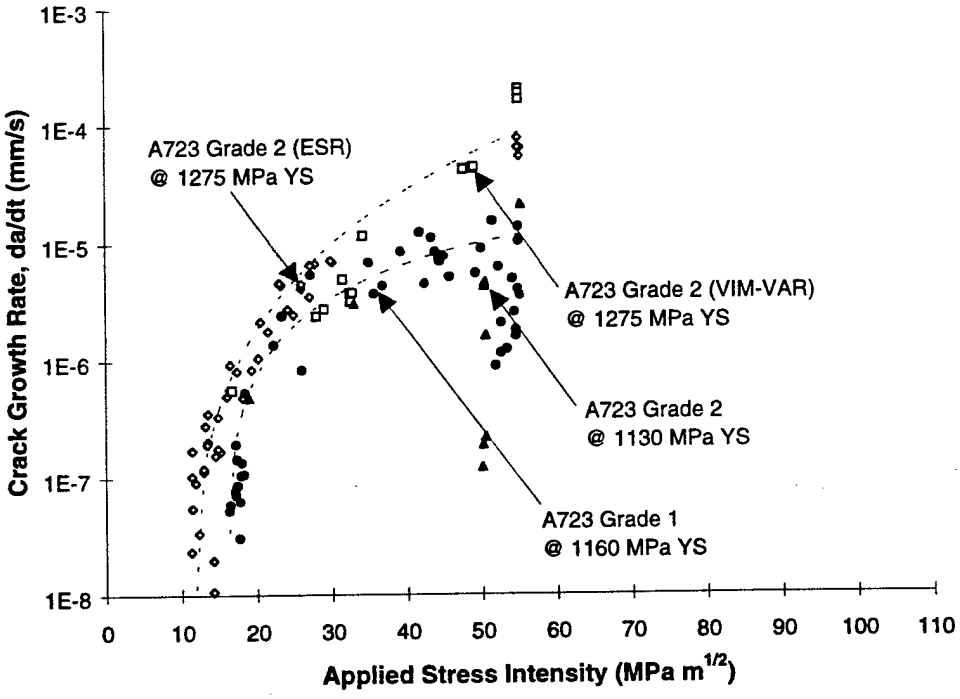

Figure 3. Crack growth rate versus applied K for A723 steel exposed to a 50% sulfuric - 50% phosphoric acid solution

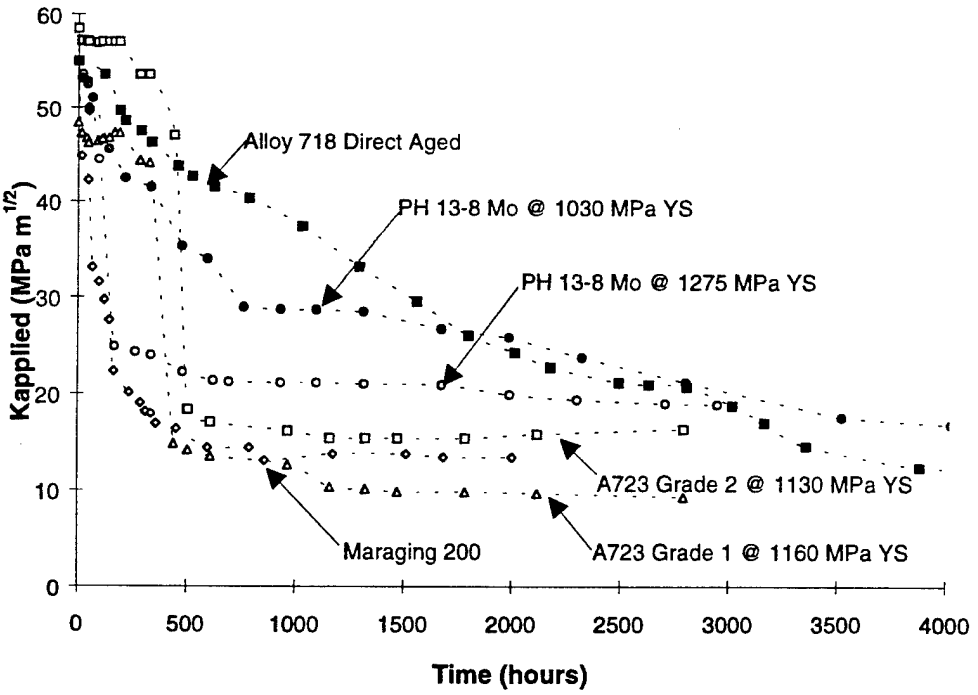

Figure 4. Applied K versus time for high-strength steels and nickel-iron base alloys tested in an electrochemical cell

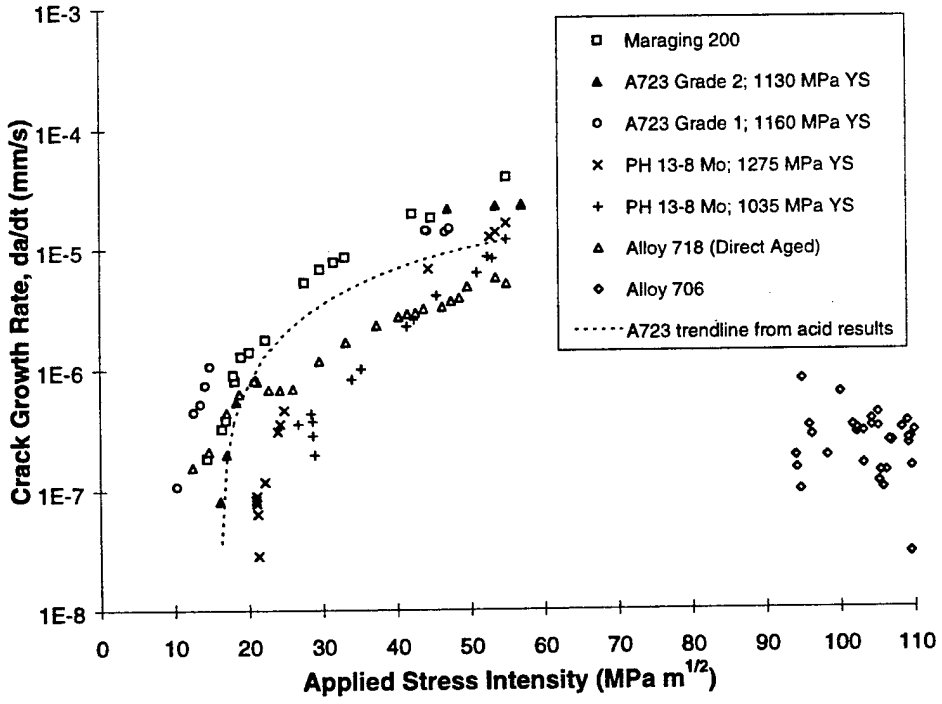

Figure 5. Crack growth rate versus applied K for high-strength steels and nickel-iron base alloys tested in an electrochemical cell

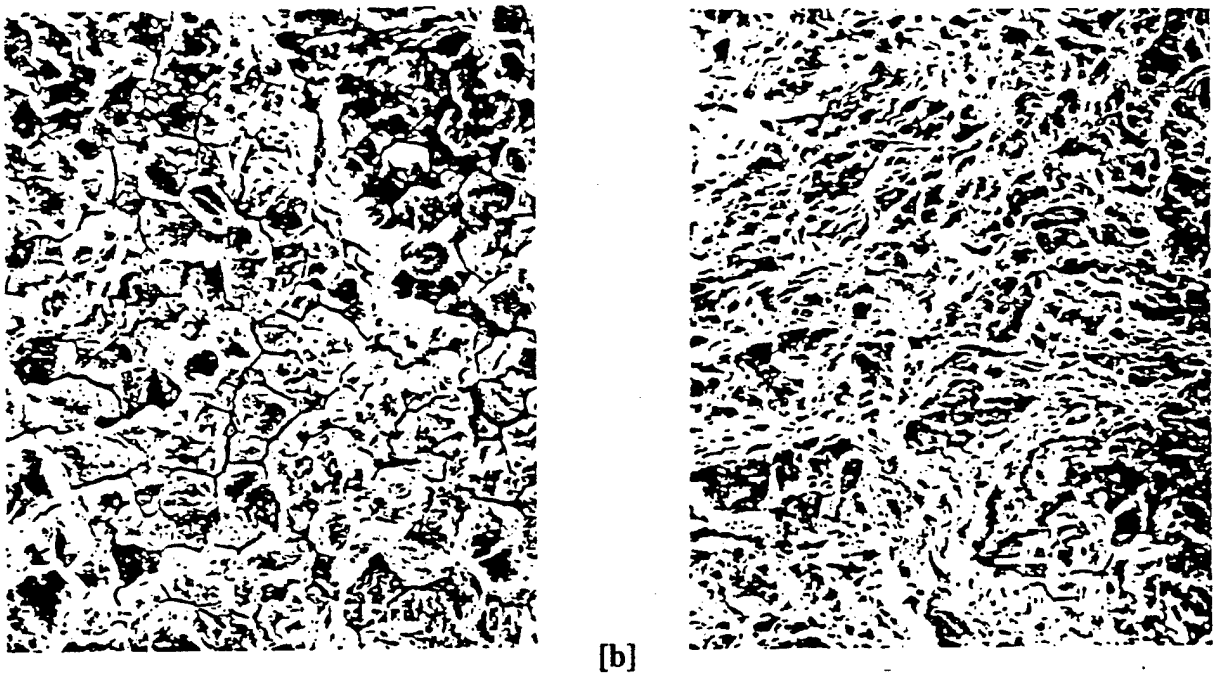

[a] [b]

Figure 6. SEM fractographs of a 1275 MPa YS A723 steel exposed to an acid solution for 1,100 hours; 750x magnification: [a] intergranular cracking near the crack tip and [b] microvoid coalescence in the ruptured remaining ligament.

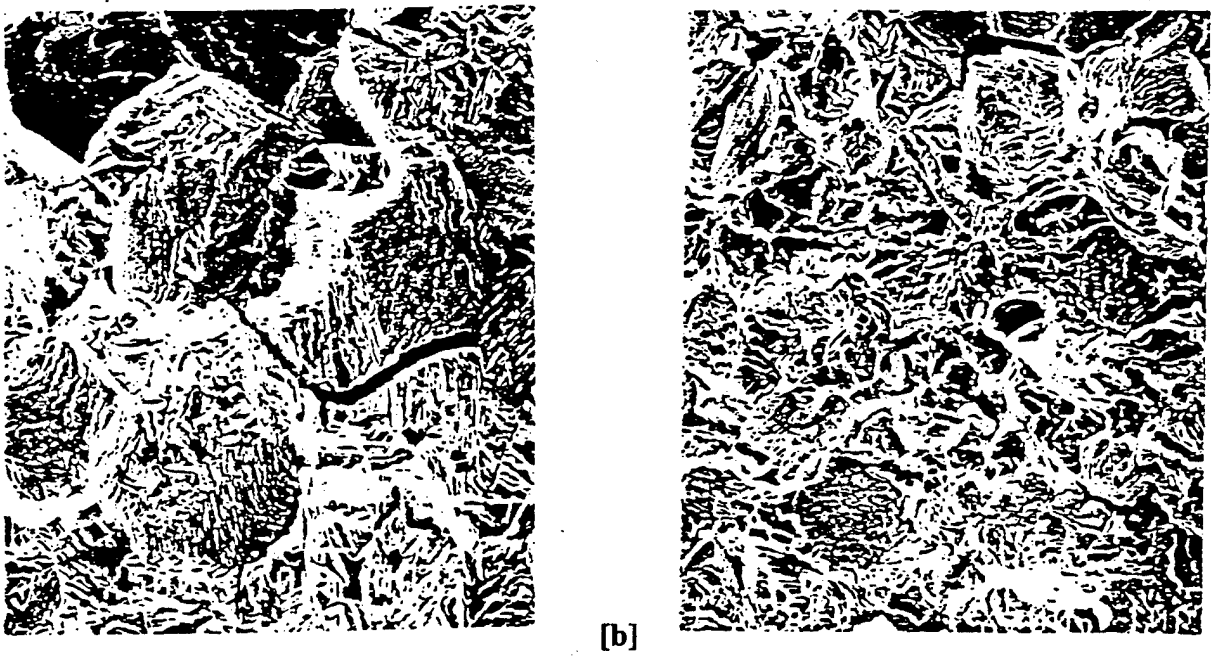

[a] [b]

Figure 7. SEM fractographs of direct-aged Alloy 718 tested in an electrochemical cell; 500x magnification: [a] intergranular cracking in the cracked portion of the specimen and [b] mixed mode failure in the ruptured remaining ligament.

TECHNICAL REPORT INTERNAL DISTRIBUTION LIST

	NO. OF COPIES
CHIEF, DEVELOPMENT ENGINEERING DIVISION	
ATTN: AMSTA-AR-CCB-DA	1
-DB	1
-DC	1
-DD	1
-DE	1
CHIEF, ENGINEERING DIVISION	
ATTN: AMSTA-AR-CCB-E	1
-EA	1
-EB	1
-EC	1
CHIEF, TECHNOLOGY DIVISION	
ATTN: AMSTA-AR-CCB-T	2
-TA	1
-TB	1
-TC	1
TECHNICAL LIBRARY	
ATTN: AMSTA-AR-CCB-O	5
TECHNICAL PUBLICATIONS & EDITING SECTION	
ATTN: AMSTA-AR-CCB-O	3
OPERATIONS DIRECTORATE	
ATTN: SIOWV-ODP-P	1
DIRECTOR, PROCUREMENT & CONTRACTING DIRECTORATE	
ATTN: SIOWV-PP	1
DIRECTOR, PRODUCT ASSURANCE & TEST DIRECTORATE	
ATTN: SIOWV-QA	1

NOTE: PLEASE NOTIFY DIRECTOR, BENÉT LABORATORIES, ATTN: AMSTA-AR-CCB-O OF ADDRESS CHANGES.

TECHNICAL REPORT EXTERNAL DISTRIBUTION LIST

	NO. OF COPIES
ASST SEC OF THE ARMY RESEARCH AND DEVELOPMENT ATTN: DEPT FOR SCI AND TECH THE PENTAGON WASHINGTON, D.C. 20310-0103	1
DEFENSE TECHNICAL INFO CENTER ATTN: DTIC-OCP (ACQUISITIONS) 8725 JOHN J. KINGMAN ROAD STE 0944 FT. BELVOIR, VA 22060-6218	2
COMMANDER U.S. ARMY ARDEC ATTN: AMSTA-AR-AEE, BLDG. 3022 AMSTA-AR-AES, BLDG. 321 AMSTA-AR-AET-O, BLDG. 183 AMSTA-AR-FSA, BLDG. 354 AMSTA-AR-FSM-E AMSTA-AR-FSS-D, BLDG. 94 AMSTA-AR-IMC, BLDG. 59 PICATINNY ARSENAL, NJ 07806-5000	 1 1 1 1 1 1 2
DIRECTOR U.S. ARMY RESEARCH LABORATORY ATTN: AMSRL-DD-T, BLDG. 305 ABERDEEN PROVING GROUND, MD 21005-5066	1
DIRECTOR U.S. ARMY RESEARCH LABORATORY ATTN: AMSRL-WT-PD (DR. B. BURNS) ABERDEEN PROVING GROUND, MD 21005-5066	1
COMMANDER ROCK ISLAND ARSENAL ATTN: SMCRI-SEM ROCK ISLAND, IL 61299-5001	1
COMMANDER U.S. ARMY TANK-AUTMV R&D COMMAND ATTN: AMSTA-DDL (TECH LIBRARY) WARREN, MI 48397-5000	1
COMMANDER U.S. MILITARY ACADEMY ATTN: DEPARTMENT OF MECHANICS WEST POINT, NY 10966-1792	1
U.S. ARMY MISSILE COMMAND REDSTONE SCIENTIFIC INFO CENTER ATTN: AMSMI-RD-CS-R/DOCUMENTS BLDG. 4484 REDSTONE ARSENAL, AL 35898-5241	2
COMMANDER U.S. ARMY FOREIGN SCI & TECH CENTER ATTN: DRXST-SD 220 7TH STREET, N.E. CHARLOTTESVILLE, VA 22901	1
COMMANDER U.S. ARMY LABCOM, ISA ATTN: SLCIS-IM-TL 2800 POWER MILL ROAD ADELPHI, MD 20783-1145	1

NOTE: PLEASE NOTIFY COMMANDER, ARMAMENT RESEARCH, DEVELOPMENT, AND ENGINEERING CENTER, BENÉT LABORATORIES, CCAC, U.S. ARMY TANK-AUTOMOTIVE AND ARMAMENTS COMMAND, AMSTA-AR-CCB-O, WATERVLIET, NY 12189-4050 OF ADDRESS CHANGES.

TECHNICAL REPORT EXTERNAL DISTRIBUTION LIST (CONT'D)

	NO. OF COPIES
COMMANDER U.S. ARMY RESEARCH OFFICE ATTN: CHIEF, IPO P.O. BOX 12211 RESEARCH TRIANGLE PARK, NC 27709-2211	1
DIRECTOR U.S. NAVAL RESEARCH LABORATORY ATTN: MATERIALS SCI & TECH DIV WASHINGTON, D.C. 20375	1
WRIGHT LABORATORY ARMAMENT DIRECTORATE ATTN: WL/MNM EGLIN AFB, FL 32542-6810	1
WRIGHT LABORATORY ARMAMENT DIRECTORATE ATTN: WL/MNMF EGLIN AFB, FL 32542-6810	1

NOTE: PLEASE NOTIFY COMMANDER, ARMAMENT RESEARCH, DEVELOPMENT, AND ENGINEERING CENTER, BENÉT LABORATORIES, CCAC, U.S. ARMY TANK-AUTOMOTIVE AND ARMAMENTS COMMAND, AMSTA-AR-CCB-O, WATERVLIET, NY 12189-4050 OF ADDRESS CHANGES.